

Bacterial Cellulose-Chitosan Composite for Prolonged-Action L-Asparaginase in Treatment of Melanoma Cells

Anastasia N. Shishparenok¹, Egor R. Petryaev², Svetlana A. Koroleva³,
Natalya V. Dobryakova¹, Igor D. Zlotnikov⁴, Elena N. Komedchikova⁵,
Olga A. Kolesnikova⁵, Elena V. Kudryashova⁴, and Dmitry D. Zhdanov^{1,a*}

¹*Institute of Biomedical Chemistry, 119121 Moscow, Russia*

²*Moscow Polytechnic University, 107023 Moscow, Russia*

³*Patrice Lumumba Peoples' Friendship University of Russia (RUDN University), 117198 Moscow, Russia*

⁴*Faculty of Chemistry, Lomonosov Moscow State University, 119991 Moscow, Russia*

⁵*Moscow Institute of Physics and Technology (National Research University),
141701 Dolgoprudny, Moscow Region, Russia*

^a*e-mail: zhdanovdd@mail.ru*

Received May 30, 2024

Revised July 12, 2024

Accepted July 22, 2024

Abstract—A significant challenge associated with the therapeutic use of L-ASP for treatment of tumors is its rapid clearance from plasma. Effectiveness of L-ASP is limited by the dose-dependent toxicity. Therefore, new approaches are being developed for L-ASP to improve its therapeutic properties. One of the approaches to improve properties of the enzymes, including L-ASP, is immobilization on various types of biocompatible polymers. Immobilization of enzymes on a carrier could improve stability of the enzyme and change duration of its enzymatic activity. Bacterial cellulose (BC) is a promising carrier for various drugs due to its biocompatibility, non-toxicity, high porosity, and high drug loading capacity. Therefore, this material has high potential for application in biomedicine. Native BC is known to have a number of disadvantages related to structural stability, which has led to consideration of the modified BC as a potential carrier for immobilization of various proteins, including L-ASP. In our study, a BC–chitosan composite in which chitosan is cross-linked with glutaraldehyde was proposed for immobilization of L-ASP. Physicochemical characteristics of the BC–chitosan films were found to be superior to those of native BC films, resulting in increase in the release time of L-ASP *in vitro* from 8 to 24 h. These films exhibited prolonged toxicity (up to 10 h) against the melanoma cell line. The suggested strategy for A-ASP immobilization on the BC–chitosan films could be potentially used for developing therapeutics for treatment of surface types of cancers including melanomas.

DOI: 10.1134/S0006297924100067

Keywords: L-asparaginase, bacterial cellulose, chitosan, kinetic models, cytotoxicity, melanoma

INTRODUCTION

L-asparaginase (L-ASP, EC3.5.1.1) is an enzyme that catalyzes hydrolysis of asparagine with formation of ammonia and L-aspartic acid. Various forms of this en-

zyme are used in pharmaceutical and food industries [1-6]. Native L-ASP of *Escherichia coli* (EcaII), asparaginase from *E. coli* conjugated with polyethylene glycol (PEG–asparaginase), and L-ASP of *Erwinia chrysanthemi* (ErA) are successfully used for treatment of acute

Abbreviations: BC, bacterial cellulose; Eca, ErA, and Ewa, therapeutic forms of L-ASP; L-ASP, L-asparaginase; SEM, scanning electron microscopy; PEG, polyethylene glycol.

* To whom correspondence should be addressed.

lymphoblastic leukaemia [7-9]. It has been shown in recent studies that L-ASP used in treatment of acute leukaemia could potentially be used for treatment of several aggressive types of solid tumors including breast cancer [10], glioblastoma, pancreatic cancer, and hepatocellular carcinoma [11]. Use of L-ASP, however, is associated with multiple side effects, short half-life time of the drug, and toxicity [12]. Period of inactivation of L-ASP reduces sharply from 18-24 h to 2.5 h due to generation of neutralizing antibodies and proteolytic degradation [13]. Therapeutic efficiency of the most often used form of L-ASP, EcAII [9], is decreased due to the relatively high glutaminase activity [14]. Glutaminase activity is associated with the development of such side effects as thrombosis, pancreatitis, hyperglycemia, and toxicity [9, 15]. In comparison with the native EcAII, the PEG-form of this enzyme exhibits longer half-life time and lower frequency of development of toxic side effects [9], nevertheless, 30% of the patients develop hypersensitivity reaction [16, 17]. Preparations based on the ErA enzyme and its homolog from *Erwinia carotovora* (EwA) were developed as the second-line therapy in the case of development of hypersensitivity to EcA [17]. ErA and EwA have lower toxicity due to the lower specificity to glutamine and, as a consequence, lower number of side effects [18, 19]. However, EwA is less active and less stable in comparison with EcA [19, 20]. Hence, development of the methods to prolong the action of L-ASP [21, 22], in particular of EwA, and decrease the number of side effects is an urgent task. One of the main approaches to solve these problems is search for new sources of L-ASP, as well as development of less immunogenic and more stable variants of L-ASP with the help of genetic engineering [6, 23].

Immobilization of L-ASP on various supports comprises another approach to increase stability, half-life time, and to decrease toxicity [24, 25]. Immobilization allows optimizing catalytic activity and minimizing side effects [26, 27]. Various supports have been used to immobilize L-ASP such as synthetic supports (PAG, polyimide, polyacrylamide), hybrid supports (PEG-albumin, PEG-chitosan, polymethyl methacrylate-starch, PEG-polyethylenimine), natural supports (carbohydrates – cellulose, dextran, starch, chitosan, chitin, and proteins – albumin, gelatin, collagen, silk fibers, and silk fibroin) [12, 28, 29]. One of the immobilization strategies involves modification of the L-ASP enzyme structure, such as covalent binding (conjugation) with PEG [24, 25] or chitosan [30, 31]. Another approach involves embedding enzyme into a protective structure or encapsulation [32]; this allows to decrease toxicity, prolong its half-life *in vivo*, increase stability, ensure targeted delivery and controlled release of the enzyme [12]. Erythrocytes, solid lipid nanoparticles, liposomes, polymers (poly lactic-co-glycolic acid, polyacrylamide,

polyaniline, and others) have been used for L-ASP encapsulation [12]. Benefits of both these strategies involve protection of the enzymes against deactivation and degradation with the help of immobilization [32]. At present the most popular approach for L-ASP immobilization is chemical modification of the enzyme via covalent binding with PEG [33]. This modification allowed increase half-life of the preparation, but, unfortunately, did not decrease side effects [21, 34].

Drug delivery systems based on bacterial cellulose (BC) attract attention of the researchers [35] due to its unique characteristics. BC displays high purity (absence of lignin typical for plant-derived cellulose), mechanical strength [36], high porosity, biocompatibility, high specific surface area and high density of the fibril network, i.e., characteristics affecting adsorption and release of a drug from the matrix [37]. BC is nontoxic [38].

Drawbacks of the non-modified BC involve low water holding capacity, and compounds adsorbed on this type of BC prone to leaching. That is why in order to achieve prolonged release of a drug, BC is subjected to various chemical modifications [39-42]. One of the promising compounds used for BC modification is chitosan [43]. High reactivity of amino groups in chitosan facilitates crosslinking via such linkers as glutaraldehyde. It has been shown previously [44-48] that crosslinking of cellulose with chitosan increases sorption capacity due to surface availability of the reactive hydroxyl groups of cellulose and amino groups of chitosan [49]. Introduction of crosslinks into the biopolymer network changes its texture, hydration and mechanical properties, as well chemical resistance to biodegradation [50]. Applicability of this approach has been confirmed by the studies on creation of chitosan-BC composites for immobilization of lipase [51, 52], albumin and fibronectin [53], controlled release of quercetin [54], quetiapine fumarate [55], and ibuprofen [43].

One of the main advantages of using BC is the possibility of targeted delivery of drugs to tumor tissues and controlled release; as a result, systemic side effects are minimized [40, 56]. In this study we developed a BC-chitosan composite for immobilization of *Erw. carotovora* L-ASP in order to prolong time of efficient cytotoxic activity against melanoma tumor cells.

MATERIALS AND METHODS

Preparation of bacterial cellulose. A *Komagataeibacter hansenii* strain (VKMP no. B-11239) was used for producing biofilms. The strain producer was cultivated in a Hestrin-Schramm medium of the following composition (per one liter): 10 g glucose (Sigma, USA); 5 g peptone (Diaem, Russia); 5 g yeast extract

(PanReac Applichem, Spain); 1.15 g citric acid monohydrate (Merck Millipore, Germany); 2.7 g Na₂HPO₄·2H₂O (PanReac Applichem). The medium was prepared with deionized water, pH was adjusted to 4.5 and autoclaved in flasks. Next, 1 ml of 90% ethanol was added to 200 ml of the medium as well as 15 ml of the medium with *K. hansenii* B-11239; 2-ml aliquots of the mixture were placed into the wells of 24-well plates (Wuxi NEST Biotechnology, China) and cultivated under static conditions at 27°C. Bacteria were grown for 48, 72, and 96 h to prepare BC films with different thickness. The obtained BC films were treated with a mixture of 0.1 M NaCl (Diaem) and 1% sodium dodecyl sulfate (Merck Millipore) for 72 h for lysing and removal of bacteria, which was followed by washing films with deionized water to remove cell residues and adjust pH to neutral.

Preparation of BC–chitosan composites. BC–chitosan composite was prepared using *ex situ* strategy [37, 57, 58]. Solutions of chitosan–HCl with mean molecular mass 7 kDa (degree of deacetylation – 80%; provided by the Federal Research Center “Fundamentals of Biotechnology”, Russian Academy of Sciences, Russia) were prepared with concentrations 0.05, 0.1, 0.5, and 1%. For this purpose, chitosan was dissolved in a 1% solution of CH₃COOH and incubated for 1 h in a water bath with temperature 50°C until complete dissolution. Wet BC membranes were dried for 20 min at 60°C to remove excess of moisture, immersed into 1 ml of chitosan solution, and incubated for 1, 2, 3, or 6 h, with constant shaking (100 rpm) at 37°C. Next, 0.5 ml of aqueous solution of 1% glutaraldehyde (pH 7.0) (neoFroxx, Germany) was added to BC membranes and incubated at 23°C for 1, 2, 3, or 4 h. BC films were lyophilized to determine their physical characteristics. For this purpose, films were frozen in a liquid nitrogen and lyophilized for 24 h at –50°C and pressure 0.07 mbar in a freeze dryer Alpha 2-4 LD, type 101042 Lab (Christ, Germany).

Determination of water content in films, their porosity and adsorption capacity. Water contents in the films was evaluated from the change in weight after lyophilization and expressed in percent (%) using equation (1):

$$\text{Water content (\%)} = \frac{A - B}{A} \cdot 100\%, \quad (1)$$

where A – weight of a wet sample; B – weight of a dry sample.

Porosity was calculated using equation suggested by Kitaoka et al. [59]. First, BC samples with water excess removed with filter paper were weighted. Next, samples were lyophilized, and films were incubated in a deionized water for 12 h at room temperature and weighted again. Porosity was calculated according to equation (2):

$$P (\%) = \frac{Q_0 - Q_1}{Q_0 - Q_2} \cdot 100\%, \quad (2)$$

where P – membrane porosity; Q₀ – weight of a wet sample (g); Q₁ – weight of a dry sample (g); Q₂ – weight (g) after 12-h incubation of the dried sample in water.

Adsorption capacity of the films was measured according the technique suggested by Wu et al. [60] by incubation of a lyophilized film sample in a HEPES buffer (50 mM (pH 8.0); Serva, Germany) for 24 h at 37°C. The following equation (3) was used for calculations:

$$\text{Adsorption capacity (\%)} = \frac{W_t - W_0}{A} \cdot 100\%, \quad (3)$$

where W₀ and W_t – sample weight before and after incubation in a buffer, respectively.

Determination of chemical composition of the films with infrared (IR) spectroscopy. IR-spectra of lyophilized samples were recorded with a Fourier transform IR-microscope MIKRA-3 (SIMEX, Russia). Spectra were recorded in an absorption mode; 36 scans were carried out with resolution 4 cm⁻¹ at 22°C in a spectral range 4000-900 cm⁻¹.

Morphology. Morphology of lyophilized BC samples and of BC–chitosan composites was examined using scanning electron microscopy (SEM). Film samples were coated with gold and examined with the help of a MAJA3 scanning electron microscope (Tescan, Czech Republic) [61]. Sample images were acquired at acceleration voltage 7 kV and 20,000× magnification.

Immobilization of L-ASP on BC. L-ASP EwA from the *Erw. carotovora* producer (595 IU/mg; molecular mass – 37 kDa; 349 amino acid residues; purity – 98.1%; isoelectric point – 8.1; GenBank ID: AAP92666.3) was provided by the laboratory of medical biotechnology of the Institute of Biomedical Chemistry [62]. L-ASP was immobilized on BC via physical adsorption in a 50-mM HEPES buffer (pH 8.0). For this purpose, BC films were immersed in 0.5 ml of the enzyme solution with concentration 0.05 mg/ml (28 IU/ml) and incubated at 4°C for 12 h. Amount of immobilized L-ASP was determined with the help of UV-VIS-spectroscopy (Aquarius CE 7400 Spectrophotometer; Cecil Instruments Ltd., Great Britain) using protocol suggested by Dawson et al. [63]. Percent of adsorbed L-ASP was determined from difference between the initial protein content and protein content in the supernatant after incubation.

Evaluation of L-ASP release. Release of L-ASP from BC–chitosan and BC films was determined by incubation in 25 ml of 50 mM HEPES (pH 8.0) without substrate for 24 h. Every hour 300-μl aliquots were sampled and enzyme activity was determined. For this purpose, 100 μl of L-asparagine solution were added

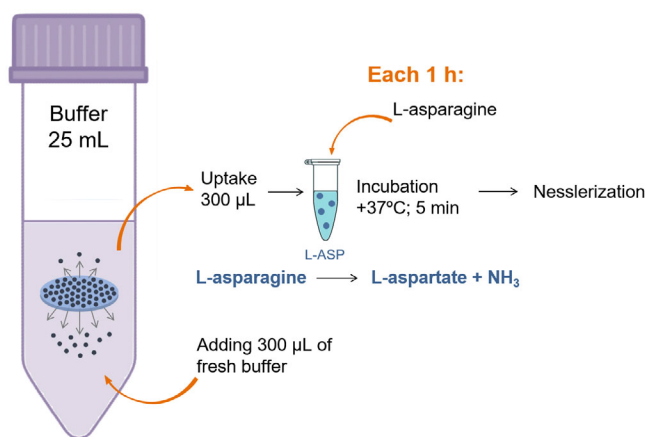


Fig. 1. Scheme of experiment for determination of L-ASP release from BC and BC-chitosan films. BC and BC-chitosan films with immobilized enzyme are incubated in 25 ml of 50 mM HEPES buffer. Immobilized L-ASP is released from films and accumulated in the buffer. Every one hour 300- μ l samples are taken (simultaneously 300 μ l of fresh buffer solution is added to maintain reaction volume) and enzyme activity is assayed by determination amount of ammonia using method of direct nesslerization after incubation with the substrate.

to the samples (40 μ M; Diaem) and the reaction mixture was incubated for 5 min at 37°C followed by determination of ammonia concentration using the method of direct Nesslerization with a Nessler reagent (PanReac Applichem, Spain) [64, 65]. Amount of enzyme that catalyzes release of 1 μ mol of ammonia per 1 min at 37°C was defined as one unit. After each sampling 300 μ l of fresh buffer was added to the reaction mixture to maintain its volume. Scheme of the experiment is presented in Fig. 1.

The data on the rate of enzyme release were used to construct kinetic models for the release: zero-order model, first-order model, Higuchi's model, Korsmeyer–Peppas model, and Hixson–Crowell model [66]. To describe the mechanism of release Korsmeyer–Peppas model was used and diffusion coefficient (n) was determined characterizing differences in the L-ASP release from BC matrices.

Evaluation of cytotoxicity. Human melanoma cell lines A375, A875, and MelJuso, as well mouse melanoma cells B16F10 (obtained from the collection of the Blokhin Russian Cancer Research Center) were cultivated in a RPMI-1640 medium (PanEco, Russia). Human fibroblast cell line WI-38 (ATCC, USA) cultivated in a DMEM medium (PanEco) was used as a conditionally normal cell line. Cultivation medium contained 5% fetal bovine serum (Capricorn Scientific, Germany) and 1% sodium pyruvate (PanEco). Cells were grown in an atmosphere of 5% CO₂ in a CO₂-incubator at 37°C. Prior to experiment cells were tested for the presence of mycoplasma with the help of a Plasmotest™ reagent kit (InvivoGen, USA).

To determine the IC₅₀ level (enzyme concentration decreasing cell viability by 50%) cell were cultivated for 72 h in a 96-well plate (Wuxi NEST Biotechnology) in the presence of free EwA in concentration range 0.01-10 U/ml. Cytotoxicity was determined using MTT test by monitoring transformation of the tetrazolium salt, 3-(4,5-dimethylthiazole-2-yl)-2,5-diphenylterazolium bromide (Serva), into formazan [67]. Formazan absorption at wavelength 540 nm was determined with the help of a SuPerMax3000 plate reader (Flash Spectrum, China). IC₅₀ values were calculated from the dependencies of cell viability on enzyme concentration [68].

To identify the cell line most sensitive to EwA immobilized on the BC-chitosan composite, cells were incubated in the presence of the composite in a 24-well plate (Wuxi NEST Biotechnology) for 24 h. Cytotoxicity was determined using MTT test after 48-h incubation with films.

To determine duration of action of the immobilized enzyme, cells of the human uveal melanoma cell line A875 and conditionally normal fibroblasts of the WI-38 cell line were seeded into a 24-well plate with density 5×10^4 cells per well and cultivated for 24 h. Next BC and BC-chitosan films with immobilized L-ASP were placed into wells and incubated for 3 h followed by transfer into new wells with cells. Cytotoxicity was evaluated 48 h after end of incubation with the films using MTT test. Optical images of cell morphology 72 h after incubation were obtained with an inverted microscope Biomed 3I (Biomed, Russia) in the bright field mode.

Statistical analysis. Quantitative data are presented as a mean \pm standard deviation of the mean calculated based on the data from three independent experiments. All data were analyzed using the MS Office Excel 2016 software (Microsoft Inc., USA). Values $p < 0.05$ were considered statistically significant.

RESULTS

Optimization of conditions of BC-chitosan composite preparation. To identify optimal condition for preparation of BC-chitosan composite the following parameters were varied: time of BC-producing bacteria cultivation, time of crosslinking of chitosan with glutaraldehyde, chitosan concentration, and time of incubation of chitosan with BC. Conditions which did not results in the loss of enzyme activity, i.e., activity of the enzyme on the BC-chitosan film was the same as on the BC film after 24 h.

Kinetics of L-ASP release from the BC and BC-chitosan films is presented in Fig. 2. The rate of L-ASP release from the BC-chitosan film (chitosan concentration 0.05%) depended on time of cultivation of BC producer, i.e., thickness and porosity of the films (Fig. 2a).

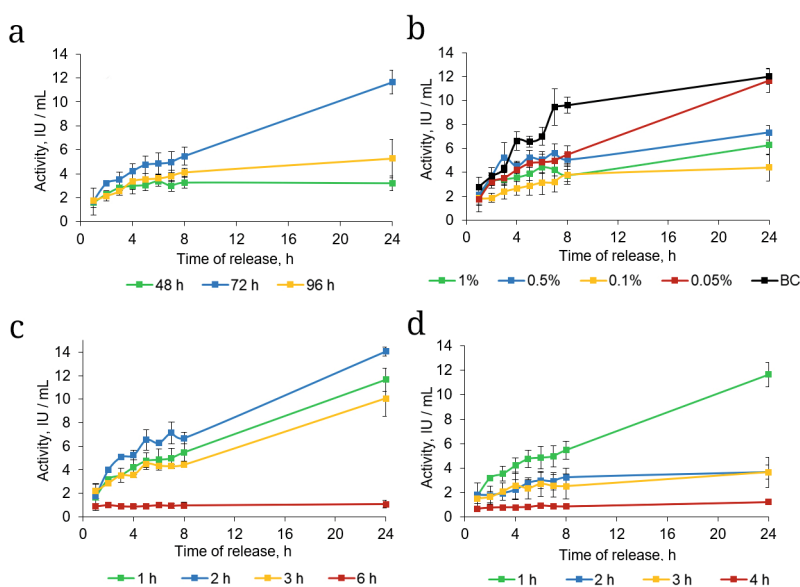


Fig. 2. Effect of condition of BC–chitosan composite preparation on the 24-h enzyme release. a) Effect of time of film growth; b) effect of chitosan concentration. Activity of enzyme immobilized on the BC films is shown in the panel for comparison. c) Effect of time of incubation with chitosan; d) effect of time of incubation with glutaraldehyde.

Maximum rate of release was observed from the films that grew for 72 h. Films grown for 48 and 96 h demonstrated 2-fold lower rate of release. Such difference could be explained by the different inner structure of the films. Addition of chitosan to BC leads to formation of three-dimensional structure, and, as a result, size of pores and adsorption capacity of the films changes. It is known that insertion of an exogenous molecule, as a rule macromolecule, changes the structure of BC fibrils, which affects size and volume of pores [69]. Hence, films grown for 72 h displayed optimal porosity characteristics for immobilization and release of L-ASP.

Chitosan concentration in the composite did not affect proportionally the rate of enzyme release (Fig. 2b). The composites with chitosan concentration 0.1, 0.5, and 1% demonstrated lower rate of the enzyme release in comparison with the composite with chitosan concentration 0.05%. Optimal time of incubation of BC with chitosan (with concentration 0.05%) was 2 h (Fig. 2c), as in this case maximum activity of the immobilized L-ASP was observed. These differences could be explained by the short time of incubation of BC in chitosan solution (2 h). In other studies [70–72] longer incubation time of BC with chitosan or another component was used, and it was shown that penetration of chitosan into BC increased significantly during the incubation period from 5 to 20 h, and after that it practically did not change [73]. Hence, chitosan concentration in the case of 1–2-h incubation of BC with chitosan does not affect the rate of L-ASP release.

It was revealed in the course of optimization of the incubation time of BC–chitosan composite with glutaraldehyde that the highest L-ASP activity after 24 h

was observed for the films with chitosan incubated with glutaraldehyde for 1 h (Fig. 2d). Increase of this incubation time to 4 h caused significant decrease of the enzyme activity, and after 24-h incubation activity of the enzyme decreased almost to zero.

Optimization of conditions for preparation of BC–chitosan composite demonstrated that optimal time of cultivation of the BC-producers for film production was 72 h, optimal concentration of chitosan – 0.05%, time of incubation with chitosan – 2 h, time of incubation of BC–chitosan with glutaraldehyde – 1 h. The films produced under these optimal conditions were used in the following experiments.

Kinetic models of drug release. The data on dynamics of L-ASP release obtained by measuring the enzyme activity were used for modeling kinetic parameters of L-ASP release from BC and BC–chitosan composites. Release from the BC–chitosan composite is best described by the Higuchi's model (Fig. 3c; Table 1),

Table 1. Regression coefficients (R^2) for kinetic models of L-ASP release for 8 h from BC and BC–chitosan films

Kinetic model	BC	BC–chitosan
Zero order model	0.960	0.928
First order model	0.959	0.948
Higuchi's model	0.937	0.971
Hixson–Crowell model	0.962	0.915
Korsmeyer–Peppas model	0.985	0.961

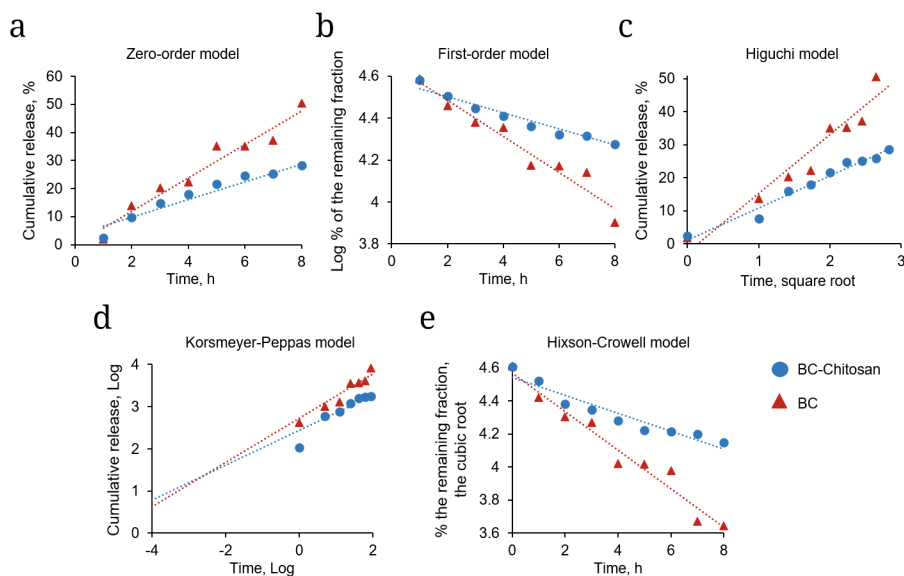


Fig. 3. Graphic representation of kinetic models for release of L-ASP immobilized on BC–chitosan composite and BC. a) Zero order model; b) First order model; c) Higuchi's model; d) Korsmeyer–Peppas model; e) Hixson–Crowell model.

in which release of a drug is controlled by diffusion exhibiting first-order dependence on concentration gradient [74]. Release from the non-modified BC corresponds to the Korsmeyer–Peppas kinetic model (Fig. 3d; Table 1), in which release of a drug is controlled by the processes of matrix relaxation and rearrangement [75].

Within first 8 h 52% of L-ASP was released from BC films, and from the BC–chitosan films – only 29% (Fig. 2b; Fig. 3a). After 24 h 65% of the enzyme was released from the BC films, and 63% – from the BC–chitosan films. These data indicate that a relatively fast release is observed from the non-modified film within first 8 h, which slows down later. The films modified with chitosan demonstrate slower, prolonged release of the enzyme without sharp release within first 8 h.

Table 2. Characteristics of BC–chitosan and BC films

Parameter	BC–chitosan	BC
Weight of a wet film, mg	401.8 ± 0.7	402.0 ± 0.9
Weight of a lyophilized film, mg	5.3 ± 0.6	3.7 ± 0.6
Weight of a film after incubation in water, mg	154.3 ± 18.2	63.7 ± 23.1
Water content, %	98.67 ± 0.14	99.09 ± 0.14
Porosity, %	160.77 ± 11.47	119.52 ± 7.95
Adsorption capacity, %	2794 ± 341	1745 ± 630

Moreover, the BC and BC–films differ in the mode of diffusion. Diffusion coefficient (n) calculated for the BC–chitosan composite for the first 8 h was 0.246 ± 0.029 , and for the BC – 0.743 ± 0.142 ($p < 0.05$). In the first case the L-ASP diffusion is described by the Fick's law ($n < 0.45$), in which the rate of diffusion is much slower than the rate of polymer matrix relaxation [76]. In the second case release of the enzyme is characterized by the non-Fickian diffusion ($0.45 < n < 0.89$). Fick's diffusion is related to the process of solute transport within the polymer with relaxation time significantly longer than the time of solute diffusion. When the time of polymer relaxation is comparable with the solute diffusion time, macroscopic release of the drug becomes abnormal or non-Fickian [77], which was observed for the case of L-ASP immobilized on BC.

Effect of BC modification on characteristics of the films. Analysis of water holding capacity of BC films before and after modification demonstrated that modification with chitosan practically does not affect water holding capacity of the films (Table 2). However, adsorption capacity for water in the BC–chitosan films after lyophilization was 1.6-fold higher than in the case of BC films. Increase of porosity of the inner structure of the BC–chitosan composite (1.34-fold) in comparison with the BC film was also revealed.

Improvement of adsorption capacity and porosity of the modified BC after lyophilization could be associated with higher melting temperature of the bound water due to lower accessibility and better water holding capacity in comparison with the control. Formation of pores depends on the number of ice crystals formed by the water adsorbed by the material. Ice crystals

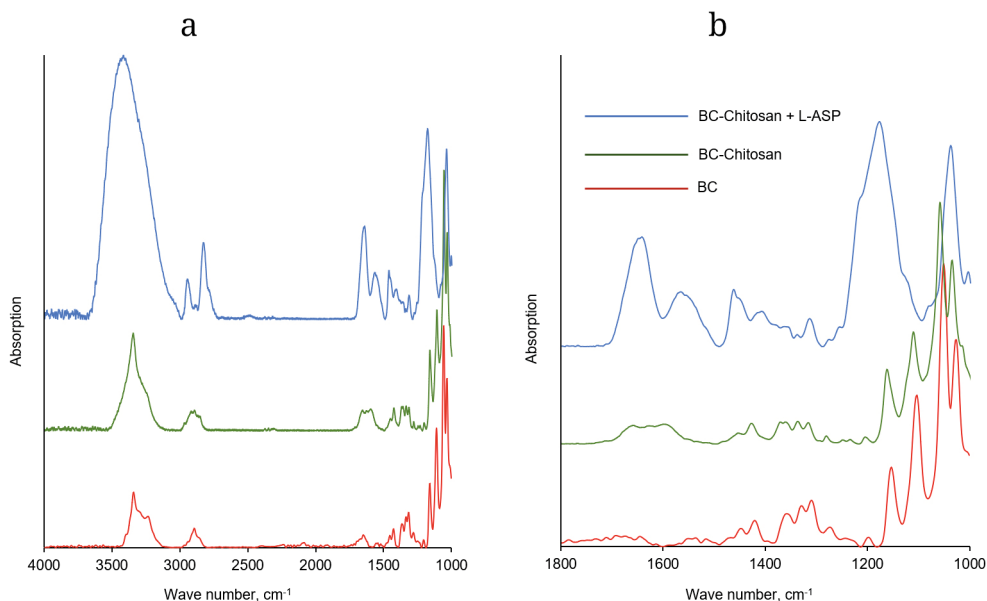


Fig. 4. IR spectra of BC–chitosan and BC films. a) Range 1000–4000 cm^{-1} ; b) range 1000–2000 cm^{-1} .

are completely sublimated in the process of drying, and the volume occupied by ice becomes a pore [78]. Higher ratios of the surface area to volume in thinner non-modified BC films leads to higher rates of formation of unbound water and its evaporation [79], which results in the lower water adsorption capacity.

IR spectra of the films. In order to determine chemical composition of the BC–chitosan and BC films used for L-ASP immobilization their infrared spectra have been recorded (Fig. 4).

The spectra of BC-based films have common peaks corresponding to cellulose: broad peak at 3335 cm^{-1} (Fig. 4a) typical for valent vibrations of $-\text{OH}$ group; peak at 2876 cm^{-1} typical for valent vibrations of aliphatic CH_2 -groups, and peak at 1435 cm^{-1} assigned to deformation vibration of $-\text{CH}$ groups [80]. The peaks observed at wavenumbers 1618, 1435, 1323, 1155, and 1066 cm^{-1} correspond to various cellulose groups: deformation vibrations of $-\text{CH}_2$ groups, deformation vibrations of $-\text{CH}$ groups, asymmetric stretching of glycosidic bonds $\text{C}-\text{O}-\text{C}$, and stretching of $\text{C}-\text{O}$ bonds, respectively (Fig. 4b).

IR spectrum of BC–chitosan films was similar to the spectrum of BC, because majority of the functional groups are common for both cellulose and chitosan [81, 82]. Peaks of valent vibrations of $-\text{OH}$ groups at 3359 cm^{-1} , $-\text{CH}$ groups at 2837 cm^{-1} , and peak of deformation vibrations at 1435 cm^{-1} typical for $\alpha\text{-CH}_2$ groups were observed (Fig. 4a) [83]. Unlike in the spectrum of BC, the spectrum of BC–chitosan has a peak of the chitosan $\text{N}-\text{H}$ groups (deacetylated amino groups, primary amino groups) at 1589 cm^{-1} (Fig. 4b). Additionally, the spectrum of the BC–chitosan composite has a peak typical from the $-\text{CH}=\text{N}-$ group observed

at $\sim 1682\text{ cm}^{-1}$, which indicated formation of the Schiff base [84]. The spectrum of the BC–chitosan film with immobilized L-ASP (Fig. 4b) also have peaks typical for amide I ($1500\text{--}1600\text{ cm}^{-1}$), amide II ($1600\text{--}1700\text{ cm}^{-1}$), and amide III ($1200\text{--}1350\text{ cm}^{-1}$). It indicated that the reaction of glutaraldehyde with primary amino groups of chitosan leading to formation of covalent crosslinks occurred in the BC–chitosan composite after incubation with glutaraldehyde [85].

Morphology of BC-based films. Cultivation of the stain producer *K. hanseii* in a 24-well plate allows producing biofilms with diameter 16 mm (Fig. 5a). Morphological changes of the BC structure before and modification were analyzed based on SEM images. Lyophilization of BC films results in generation of void spaces in the network organization, which determine final porous structure [71]. Microstructures of BC- and BC–chitosan films are shown in Fig. 5. The BC–chitosan films (Fig. 5b) form more ordered porous layered structure with large number of pores of smaller size in comparison with BC films (Fig. 5c). The BC nanofibers in BC–chitosan films are intertwined and folded forming a denser structure in comparison with the loosely arranged fibers in BC films. Therefore, different degree of density of the three-dimensional network in BC and BC–chitosan could affect swelling, adsorption capacity, and rate of L-ASP release.

Prolonged cytotoxic action of L-ASP immobilized on BC–chitosan films. To select cells most sensitive to the action of L-ASP the IC_{50} values for the native EwA enzyme were determined. Among the melanoma cell lines, the cells of A875 cell line were shown to be most sensitive, and the cells of A375 cell line were shown to be the least sensitive (Table 3). As expected,

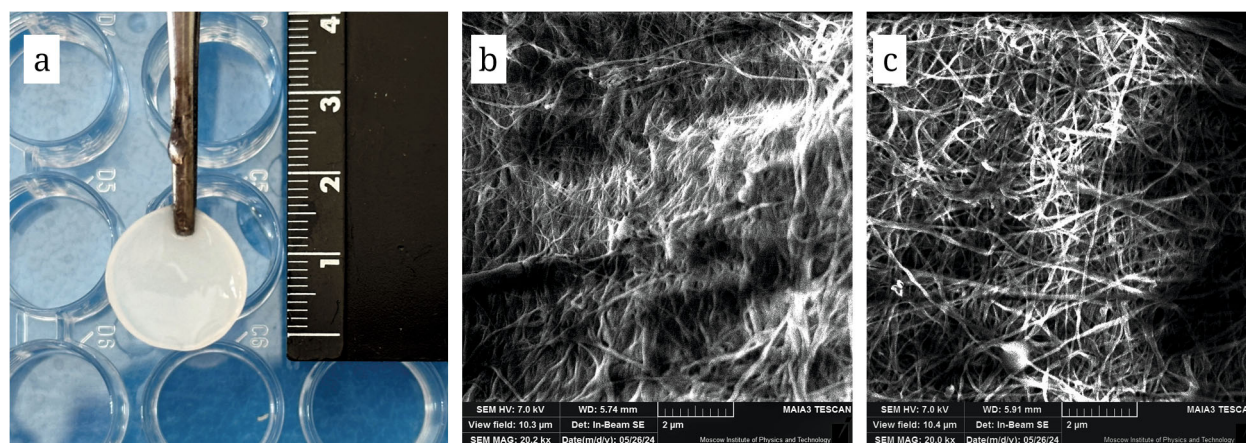


Fig. 5. Film morphology. a) Appearance of BC film grown in a well of 24-well plate. b) SEM image of cross section of BC–chitosan film. c) SEM image of cross section of BC film.

the control fibroblasts of the WI-38 cell line were the most resistant to the enzyme action.

Toxicity of L-ASP released from the film is determined by the rate of enzyme release and rate of enzyme degradation, i.e., by the amount of active enzyme in the medium. In order to identify cell line most sensitive to EwA immobilized on the BC–chitosan composite, survival of cells after 24-h incubation with the films was determined. The survival data were in good agreement with the IC_{50} values. The most sensitive melanoma cells were the cells of A875 cell line, and the least sensitive – cells of the A375 cell line (Table 3). The conditionally normal fibroblasts WI-38 were the most resistant and demonstrated the highest viability.

To evaluate duration of the action of L-ASP immobilized on BC or BC–chitosan on the A875 melanoma cells and on the conditionally normal fibroblasts the study was conducted involving transfer of the cells every 3 h into the new wells with the cells (Figs. 6 and 7). The enzyme immobilized on the BC films modified with chitosan preserved its cytotoxicity activity even after four sequential incubations with the cells

Table 3. IC_{50} values for free EwA and survival of cells after incubation with EwA immobilized on BC–chitosan films

Cell line	IC_{50} , U/ml	Survival, % of control
A875	0.04	11.49 ± 6.93
MelJuso	0.12	22.89 ± 2.66
B16F10	0.24	34.26 ± 6.92
A375	0.38	50.81 ± 10.51
WI-38	8.22	93.61 ± 17.24

(Fig. 6). After 6 h of incubation viability of tumor cells was ~50%, and after 12 h – 80%. At the same time enzyme in the BC film did not exhibit cytotoxic activity after the first incubation with the cells, and already after 3 h of incubation viability of the cells was at the level of control cells not treated with L-ASP. Hence, immobilization of L-ASP on the BC–chitosan composite facilitates its prolonged action on the melanoma tumor cells.

As expected, the EwA enzyme immobilized on the films, practically did not exhibit any cytotoxic effect on the conditionally normal fibroblasts WI-38 (Fig. 7). Slight decrease in the cell viability was observed only during the first 3-h incubation to the level of 66.5–85.4% for the EwA, immobilized on BC, and to the level of 71.7–93.0% for the enzyme immobilized on the BC–chitosan film.

Hence, immobilization of L-ASP on the BC–chitosan composite facilitates prolonged action of the enzyme on the tumor melanoma cells. No prolonged action on the conditionally normal cell was observed.

DISCUSSION

Despite the unique properties of native BC, its application as a support of therapeutic agents is limited by the profiles of adsorption and release of a therapeutic agent. Very often high rate of these processes is limited to the few first hours [37, 70, 86, 87]. In some cases, this could result in the initial local high accumulation of the drug and cause toxic effects in the cells from normal tissues [88].

Up to now several composites (semi-penetrable hydrogels) based on BC and chitosan with improved mechanical and antibacterial properties have been developed [43, 51, 55, 89]. Hydrogels are usually prepared by mixing BC with chitosan solution followed

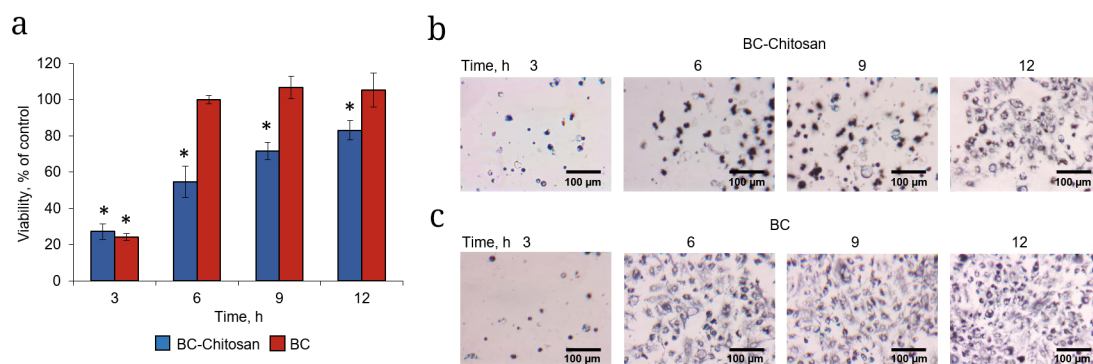


Fig. 6. Duration of cytotoxic action of L-ASP immobilized on BC and BC-chitosan films on A875 melanoma cells. a) Viability of cells evaluated with MTT-test after incubation with films and sequential transfer every 3 h to new wells. Bright-field microphotographs of the cells synthesizing formazan crystals after incubation with BC-chitosan films (b) and BC films (c) with immobilized L-ASP. * $p \leq 0.05$ in comparison with the control cells incubated with BC or BC-chitosan films not containing L-ASP.

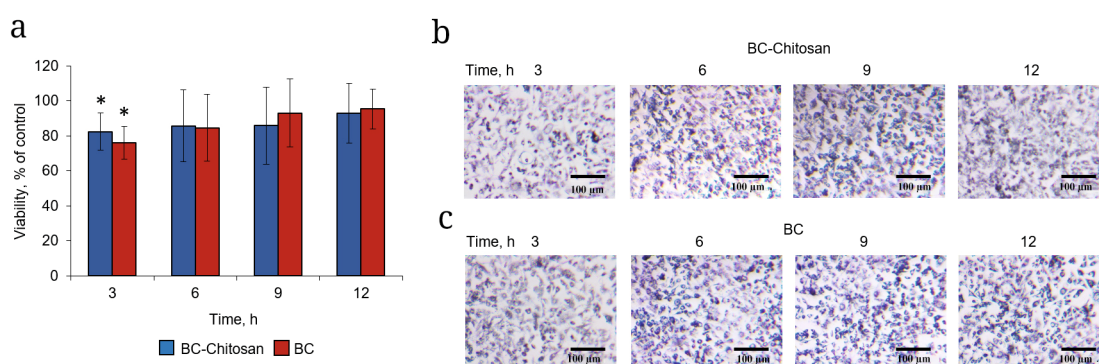


Fig. 7. Duration of cytotoxic action of L-ASP immobilized on the BC and BC-chitosan films on the conditionally normal fibroblasts of the WI-38 cell line. a) Viability of the cells measured using MTT-test after incubation with the films and sequential transfer of the films to new well after each 3 h. Bright-field microphotographs of the cells synthesizing formazan crystals after incubation with BC-chitosan (a) and BC (b) films with immobilized L-ASP. * $p \leq 0.05$ in comparison with the control cell incubated with BC or BC-chitosan films not containing L-ASP.

by crosslinking with glutaraldehyde. In this system one polymer is crosslinked and another polymer remains linear. However, the linear polymer remains physically bound with the crosslinked polymer via Van-der-Waals forces, electrostatic interactions, hydrogen bonds, or combination of these interactions [89]. It is known that crosslinking of hydrogels could prevent premature proteolytic degradation of immobilized highly labile macromolecules (such as antibodies), which could facilitate increase of half-life of a drug in blood and improve stability of hydrogels via increasing density of crosslinks [90].

It was observed in our study that the BC films grown for 96 h released L-ASP slower than the films grown for 72 h, which was comparable with the release from the films grown for 48 h (Fig. 2a). This result is in agreement with the results reported by Pavaloiu et al. [43], in which the polyvinyl alcohol-chitosan-BC composites were used to achieve controlled release of ibuprofen. Ibuprofen diffusion decreases with increase of BC concentration in the film composition. In our case it indicates that the thickness of BC

films (which depends on the time of cultivation of the producer) affects significantly the 24-h L-ASP release: activity of the films grown for 72 h was 2-fold higher than of the films grown for 48 or 96 h.

Analysis of the L-ASP release from the BC and BC-chitosan films revealed that chitosan concentration did not affect L-ASP activity (Fig. 2b; Fig. 3). This could be explained by the fact that the chitosan particles could aggregate, and chitosan was not able to completely penetrate the BC film. This hypothesis received an indirect confirmation in the study by Li et al. [72], where it was shown that adsorption capacity of the BC-hyaluronic acid composite did not depend on concentration of the latter in the first hours of incubation.

Previously, the BC-chitosan composites were mainly developed as wound dressing materials [91, 92]; and BC with chitosan were incubated for 6-12 h. We suggested to optimize time of chitosan incubation with BC for creation of L-ASP delivery agent to melanoma tumor cell. Prolonged incubation time of BC with chitosan (6 h) (Fig. 2c) resulted in the decrease of released L-ASP activity practically to zero, while incubation

of BC with chitosan for 1-2 h did not affect activity of L-ASP released after 24 h. This indicates that for immobilization of the investigated enzyme the time of incubation of BC with chitosan should be significantly reduced.

Moreover, the released enzyme activity was affected by the time of incubation of BC–chitosan with glutaraldehyde (Fig. 2d). Conditions of the reaction of glutaraldehyde with chitosan have been optimised in the earlier study by Monteiro et al. [85]. The reaction was carried out in neutral medium, and time of incubation was 1 h at room temperature. Hence, these conditions are suitable for preparation of the BC–chitosan composite for immobilization of L-ASP.

Evaluation of the L-ASP release from the BC–chitosan composite (chitosan concentration 0.05%) revealed that the cumulative release for 24 h in this case was more prolonged than in the case of native BC films. These data are in agreement with the results of application of BC–chitosan composite hydrogel beads for immobilization of lipase from *Candida rugosa* [51]. As a result of immobilization half-life of lipase increased more than 3-fold. Crosslinking of chitosan with glutaraldehyde resulted in formation of additional three-dimensional structure of the BC fibers, which caused increase of the fiber thickness (confirmed by the SEM images in Fig. 5) and more effective retention of L-ASP in the composite.

The data on the pattern of L-ASP release from the BC films or from the composite, as well application of the Higuchi's kinetic model and diffusion coefficient of the value $n < 0.45$ indicate that the enzyme release is controlled by diffusion [93]. The Higuchi's kinetic model suggests that the release of a drug obeys the Fick's law of diffusion, where the main result is dependence of the drug transport on the square root of time [94, 95]. At the same time, the release of L-ASP from the non-modified BC films was better described by the Korsmeyer–Peppas model for which abnormal diffusion ($n > 0.45$) with characteristics of subdiffusion [96] is typical, as well as faster release of L-ASP within first hours.

Diffusion of a compound is closely associated with the structure of a material through which the diffusion occurs [95], hence, modification of BC with chitosan allowed achieving prolonged release of L-ASP. Adsorption capacity of a protein on BC is affected by such characteristics as its porosity and density of fibers, which, in turn, depend on time of cultivation of the producer and composition of the culture medium [97]. In our study porosity of the BC–chitosan composite was 1.6-fold higher than in the case of non-modified BC, and following crosslinking with glutaraldehyde facilitated pore size decrease. This created steric hindrance for fast release of the enzyme from the matrix and prolonged action on the cells *in vitro*. The most

important feature of the films is the size of pores formed by the BC fibrils. The size affects steric interaction between BC and a therapeutic agent, which eventually determines how the drug is released from the matrix [90]. The effect of steric hindrance blocks the drug inside the network until the moment of the network disruption or the pore size increase due to swelling or deformation [98].

The data obtained for the cells (Fig. 6) corresponded to the general trend of L-ASP release from BC and BC–chitosan composite in solution. The immobilized enzyme exerted cytotoxic effect on the tumor cells of uveal melanoma A875, and the use of the BC–chitosan composite prolonged cytotoxic action to four sequential incubations. This indicates that even in the case of several transfers of the composite films, small amount of the released L-ASP was sufficient for cytotoxic effect, while practically 100% of L-ASP was released from the BC films during the first incubation. No prolonged cytotoxic effect was observed in the case of conditionally normal WI38 cells. Cytotoxic activity of free L-ASP was demonstrated in the recent studies for several solid tumor cell cultures [99], and the PEG-L-ASP preparation exhibited good antitumor activity against the malignant melanoma in the phase I clinical trials [100]. The EwA conjugated with PEG [22], albumin [101], glycol–chitosan [102], and PEG–chitosan [103] have been developed previously. The EwA conjugates with PEG–chitosan demonstrated 3-5-fold higher specific activity against the K562 and Jurkat cells, and composition and structure of the conjugate essentially affected the degree of cytotoxic effect [103]. At present the randomized clinical trial of the efficiency of L-ASP preparation encapsulated into erythrocytes for treatment of triple-negative breast cancer is underway [104]. Furthermore, it is known that switching to alternative types of L-ASP is recommended for the patients with hypersensitivity, immune or proteolytic inactivation of the enzyme [105]. Melanomas represent surface type of cancer, which are treated efficiently with surgical treatments [106]. However, there are clinically and genetically different subgroups of melanomas for which surgical interventions are inefficient [106, 107], which makes development of new strategies for treatment of certain types melanomas very important. That is why melanoma cell lines were selected for this study.

Some traditional methods for melanoma treatment were proved to be inefficient, which promoted investigation of combination approaches for treatment of this disease [106]. Therapy based on depletion of amino acids with the help of enzyme cleaving amino acids could be potentially used for treatment of various types of tumors [108], including melanomas. This effect on melanoma has been demonstrated for such enzymes as arginine deiminase and arginase [109].

Several systems for drug delivery to the cells with minimal side effects have been developed. One of the types of supports for these drug delivery systems are hydrogels based on natural and synthetic polymers [110]. Transdermal drug delivery has several advantages in comparison with injection of proteins into systemic blood flow – these include non-invasiveness, prevention of first-pass metabolism, prolonged and controlled action, decrease of the frequency of drug administration, improved bioavailability, simplicity of administration by the patient [111, 112]. Delivery of EwA with the help of BC could allow increasing EwA concentration at the tumor site, and also could be an alternative treatment for the patients, who cannot be treated surgically or have contraindication for systemic chemotherapy. However, this approach has a number of limitations. Epidermis acts as a barrier for large molecules, including proteins [113]. Another limitation is the fact that L-ASP immobilized on BC films could be applied only for treatment of surface tumors. Such tumor cells could become resistant to L-ASP due to the high expression asparagine synthetase, which would require therapy with higher doses of L-ASP [114]. Determination of the level of asparagine synthetase expression [109] in the cells prior to therapy could help to determine potential sensitivity of the cells to this enzyme.

Hence, localized continuous release of EwA L-ASP could be potentially beneficial for treatment of solid tumors providing prolonged local cytotoxic effect on melanoma tumor cells with decreased frequency of the drug administration.

CONCLUSIONS

Commonly known mechanism of L-ASP cytotoxicity is asparagine hydrolysis. However, alternative mechanisms such as suppression of telomerase [115-117], release of the 2-HS glycoprotein fetuin [118], and degradation of conovaline receptors [119] could also be involved in the development of cytotoxic effects. Wide spectrum of the known producers of various forms of L-ASP with different individual characteristics, primarily thermophilic organisms [120-122], as well approaches to generation of recombinant analogues of this enzyme make it possible to produce biofilms with pre-set characteristics of their biological actions [6]. New BC–chitosan composites were successfully produced by mixing chitosan suspension with BC membranes followed by crosslinking with the help of glutaraldehyde. In comparison with the non-modified films, the BC–chitosan composites have higher porosity, water holding capacity, and smaller average pore size. L-ASP from *Erw. carotovora* immobilized on the BC–chitosan composites exhibited 3-fold longer release

and maintained its cytotoxic properties against melanoma cells, but did not affect conditionally normal fibroblasts (even after three consecutive transfers), while toxicity of the films with L-ASP immobilized on BC was observed only in the course of first incubation with the cells.

Acknowledgments. The authors are grateful to Viktoriya Olegovna Shipunova (Moscow Institute of Physics and Technology) for help in acquiring SEM images and to Andrei Fedorovich Kozlov (Orekhovich Research Institute of Biomedical Chemistry) for help in lyophilization of films. Equipment purchased with the support of the Program of Lomonosov Moscow University Development (Fourier transform IR-microscope MIKTRAN-3) was used in the study.

Contributions. A.N.S. concept of the study, design and conducting experiments on modification of the films and analysis of cytotoxicity, writing draft of the paper; E.R.P. and S.A.K. conducting experiments on investigation of the enzyme release; E.N.K. and O.A.K. obtaining SEM images; N.V.D., I.D.Z., and E.V.K. experiments with IR spectroscopy; D.D.Z. concept of the study, general supervision of the work, attracting funding, editing of the final version of the paper.

Funding. This work was financially supported by the Program of Fundamental Scientific Studies in the Russian Federation for the prolonged period (2021-2030) (project no. 122022800499-5).

Ethics declarations. This work does not contain any studies involving human and animal subjects. The authors of this work declare that they have no conflicts of interest.

REFERENCES

1. Pokrovskaya, M. V., Pokrovsky, V. S., Aleksandrova, S. S., Sokolov, N. N., and Zhdanov, D. D. (2022) Molecular analysis of L-asparaginases for clarification of the mechanism of action and optimization of pharmacological functions, *Pharmaceutics*, **14**, 599, <https://doi.org/10.3390/pharmaceutics14030599>.
2. Castro, D., Marques, A. S. C., Almeida, M. R., de Paiva, G. B., Bento, H. B. S., Pedrolli, D. B., Freire, M. G., Tavares, A. P. M., and Santos-Ebinuma, V. C. (2021) L-asparaginase production review: bioprocess design and biochemical characteristics, *Appl. Microbiol. Biotechnol.*, **105**, 4515-4534, <https://doi.org/10.1007/s00253-021-11359-y>.
3. Chand, S., Mahajan, R. V., Prasad, J. P., Sahoo, D. K., Mihooliya, K. N., Dhar, M. S., and Sharma, G. (2020) A comprehensive review on microbial L-asparaginase: bioprocessing, characterization, and industrial applications, *Biotechnol. Appl. Biochem.*, **67**, 619-647, <https://doi.org/10.1002/bab.1888>.

4. Suresh, S. A., Ethiraj, S., and Rajnish, K. N. (2022) A systematic review of recent trends in research on therapeutically significant L-asparaginase and acute lymphoblastic leukemia, *Mol. Biol. Rep.*, **49**, 11281-11287, <https://doi.org/10.1007/s11033-022-07688-4>.
5. Jia, R., Wan, X., Geng, X., Xue, D., Xie, Z., and Chen, C. (2021) Microbial L-asparaginase for application in acrylamide mitigation from food: current research status and future perspectives, *Microorganisms*, **9**, 1659, <https://doi.org/10.3390/microorganisms9081659>.
6. Shishparenok, A. N., Gladilina, Y. A., and Zhdanov, D. D. (2023) Engineering and expression strategies for optimization of L-asparaginase development and production, *Int. J. Mol. Sci.*, **24**, 15220, <https://doi.org/10.3390/ijms242015220>.
7. Chan, W. K., Horvath, T. D., Tan, L., Link, T., Harutyunyan, K. G., Pontikos, M. A., Anishkin, A., Du, D., Martin, L. A., Yin, E., Rempe, S. B., Sukharev, S., Konopleva, M., Weinstein, J. N., and Lorenzi, P. L. (2019) Glutaminase activity of L-Asparaginase contributes to durable preclinical activity against acute lymphoblastic leukemia, *Mol. Cancer Ther.*, **18**, 1587-1592, <https://doi.org/10.1158/1535-7163.MCT-18-1329>.
8. Tsegaye, K., Tsehai, B. A., and Getie, B. (2024) Desirable L-asparaginases for treating cancer and current research trends, *Front. Microbiol.*, **15**, 1269282, <https://doi.org/10.3389/fmicb.2024.1269282>.
9. Liu, W., Wang, H., Wang, W., Zhu, M., Liu, C., Wang, J., and Lu, Y. (2016) Use of PEG-asparaginase in newly diagnosed adults with standard-risk acute lymphoblastic leukemia compared with *E. coli*-asparaginase: a retrospective single-center study, *Sci. Rep.*, **6**, 39463, <https://doi.org/10.1038/srep39463>.
10. Mazloun-Ravasan, S., Madadi, E., Mohammadi, A., Mansoori, B., Amini, M., Mokhtarzadeh, A., Baradaran, B., and Darvishi, F. (2021) *Yarrowia lipolytica* L-asparaginase inhibits the growth and migration of lung (A549) and breast (MCF7) cancer cells, *Int. J. Biol. Macromol.*, **170**, 406-414, <https://doi.org/10.1016/j.ijbiomac.2020.12.141>.
11. Van Trimont, M., Peeters, E., De Visser, Y., Schalk, A. M., Mondelaers, V., De Moerloose, B., Lavie, A., Lammens, T., Goossens, S., and Van Vlierberghe, P. (2022) Novel insights on the use of L-asparaginase as an efficient and safe anti-cancer therapy, *Cancers (Basel)*, **14**, 902, <https://doi.org/10.3390/cancers14040902>.
12. Talluri, V. P., Mutaliyeva, B., Sharipova, A., Ulaganathan, V., Lanka, S. S., Aidarova, S., Suigenbayeva, A., and Tleuova, A. (2023) L-Asparaginase delivery systems targeted to minimize its side-effects, *Adv. Colloid Interface Sci.*, **316**, 102915, <https://doi.org/10.1016/j.cis.2023.102915>.
13. Bahreini, E., Aghaiypour, K., Abbasalipourkabir, R., Mokarram, A. R., Goodarzi, M. T., and Saidijam, M. (2014) Preparation and nanoencapsulation of L-asparaginase II in chitosan-tripolyphosphate nanoparticles and *in vitro* release study, *Nanoscale Res. Lett.*, **9**, 340, <https://doi.org/10.1186/1556-276X-9-340>.
14. Aghaeepoor, M., Akbarzadeh, A., Mirzaie, S., Hadian, A., Jamshidi Aval, S., and Dehnavi, E. (2018) Selective reduction in glutaminase activity of L-Asparaginase by asparagine 248 to serine mutation: a combined computational and experimental effort in blood cancer treatment, *Int. J. Biol. Macromol.*, **120**, 2448-2457, <https://doi.org/10.1016/j.ijbiomac.2018.09.015>.
15. Chan, W. K., Lorenzi, P. L., Anishkin, A., Purwaha, P., Rogers, D. M., Sukharev, S., Rempe, S. B., and Weinstein, J. N. (2014) The glutaminase activity of L-asparaginase is not required for anticancer activity against ASNS-negative cells, *Blood*, **123**, 3596-3606, <https://doi.org/10.1182/blood-2013-10-535112>.
16. Rizzari, C., Mörcke, A., Valsecchi, M. G., Conter, V., Zimmermann, M., Silvestri, D., Attarbaschi, A., Niggli, F., Barbaric, D., Stary, J., Elitzur, S., Cario, G., Vinti, L., Boos, J., Zucchetti, M., Lanvers-Kaminsky, C., von Stackelberg, A., Biondi, A., and Schrappe, M. (2023) Incidence and characteristics of hypersensitivity reactions to PEG-asparaginase observed in 6136 children with acute lymphoblastic leukemia enrolled in the AIEOP-BFM ALL 2009 study protocol, *HemaSphere*, **7**, e893, <https://doi.org/10.1097/HS9.0000000000000893>.
17. Figueiredo, L., Cole, P. D., and Drachtman, R. A. (2016) Asparaginase *Erwinia chrysanthemi* as a component of a multi-agent chemotherapeutic regimen for the treatment of patients with acute lymphoblastic leukemia who have developed hypersensitivity to *E. coli*-derived asparaginase, *Expert Rev. Hematol.*, **9**, 227-234, <https://doi.org/10.1586/17474086.2016.1142370>.
18. Ko, R. H., Jones, T. L., Radvinsky, D., Robison, N., Gaynon, P. S., Panosyan, E. H., Avramis, I. A., Avramis, V. I., Rubin, J., Ettinger, L. J., Seibel, N. L., and Dhall, G. (2015) Allergic reactions and anti-asparaginase antibodies in children with high-risk acute lymphoblastic leukemia: a children's oncology group report, *Cancer*, **121**, 4205-4211, <https://doi.org/10.1002/cncr.29641>.
19. Papageorgiou, A. C., Posypanova, G. A., Andersson, C. S., Sokolov, N. N., and Krasotkina, J. (2008) Structural and functional insights into *Erwinia carotovora* L-asparaginase, *FEBS J.*, **275**, 4306-4316, <https://doi.org/10.1111/j.1742-4658.2008.06574.x>.
20. Faret, M., de Morais, S. B., Zanchin, N. I. T., and de Souza, T. (2019) L-Asparaginase from *Erwinia carotovora*: insights about its stability and activity, *Mol. Biol. Rep.*, **46**, 1313-1316, <https://doi.org/10.1007/s11033-018-4459-2>.
21. Singh, M., Hassan, N., Verma, D., Thakur, P., Panda, B. P., Panda, A. K., Sharma, R. K., Mirza, A., Mansoor, S., Alrokayan, S. H., Khan, H. A., Ahmad, P., and Iqbal, Z. (2020) Design of expert guided investigation of native L-asparaginase encapsulated long-acting cross-linker-free poly (lactic-co-glycolic) acid nanoformulation in

- an Ehrlich ascites tumor model, *Saudi Pharm. J.*, **28**, 719-728, <https://doi.org/10.1016/j.jsps.2020.04.014>.
22. Melik-Nubarov, N. S., Grozdova, I. D., Lomakina, G. Y., Pokrovskaya, M. V., Pokrovski, V. S., Aleksandrova, S. S., Abakumova, O. Y., Podobed, O. V., Grishin, D. V., and Sokolov, N. N. (2017) PEGylated recombinant L-asparaginase from *Erwinia carotovora*: production, properties, and potential applications, *Appl. Biochem. Microbiol.*, **53**, 165-172, <https://doi.org/10.1134/S0003683817020119>.
 23. Fonseca, M. H. G., da Silva Fiúza, T., de Morais, S. B., Souza, T., and de Trevizani, R. (2021) Circumventing the side effects of L-asparaginase, *Biomed. Pharmacother.*, **139**, 111616, <https://doi.org/10.1016/j.biopha.2021.111616>.
 24. Meneguetti, G. P., Santos, J. H. P. M., Obreque, K. M. T., Barbosa, C. M. V., Monteiro, G., Farsky, S. H. P., Marim de Oliveira, A., Angeli, C. B., Palmisano, G., Ventura, S. P. M., Pessoa-Junior, A., and de Oliveira Rangel-Yagui, C. (2019) Novel site-specific PEGylated L-asparaginase, *PLoS One*, **14**, e0211951, <https://doi.org/10.1371/journal.pone.0211951>.
 25. Feenstra, L. R., Gehring, R., van Geijlswijk, I. M., König, T., Prinsen, H. C. M. T., Vandemeulebroecke, K., Lammens, T., Krupa, A., and Teske, E. (2022) Evaluation of PEG-L-asparaginase in asparagine suppression and anti-drug antibody development in healthy Beagle dogs: a multi-phase preclinical study, *Vet. J.*, **286**, 105854, <https://doi.org/10.1016/j.tvjl.2022.105854>.
 26. Mohamad, N. R., Marzuki, N. H. C., Buang, N. A., Huyop, F., and Wahab, R. A. (2015) An overview of technologies for immobilization of enzymes and surface analysis techniques for immobilized enzymes, *Biotechnol. Biotechnol. Equip.*, **29**, 205-220, <https://doi.org/10.1080/13102818.2015.1008192>.
 27. Zhang, D.-H., Yuwen, L.-X., and Peng, L.-J. (2013) Parameters affecting the performance of immobilized enzyme, *J. Chem.*, **2013**, 946248, <https://doi.org/10.1155/2013/946248>.
 28. Ulu, A., and Ates, B. (2017) Immobilization of L-asparaginase on carrier materials: a comprehensive review, *Bioconjug. Chem.*, **28**, 1598-1610, <https://doi.org/10.1021/acs.bioconjchem.7b00217>.
 29. Dobryakova, N. V., Zhdanov, D. D., Sokolov, N. N., Aleksandrova, S. S., Pokrovskaya, M. V., and Kudryashova, E. V. (2023) *Rhodospirillum rubrum* L-asparaginase conjugates with polyamines of improved biocatalytic properties as a new promising drug for the treatment of leukemia, *Appl. Sci.*, **13**, 3373, <https://doi.org/10.3390/app13053373>.
 30. Qian, G., Zhou, J., Ma, J., He, B., and Wang, D. (1997) Chemical modification of L-asparaginase with N, O-carboxymethyl chitosan and its effects on plasma half-life and other properties, *Sci. China Ser. B Chem.*, **40**, 337-341, <https://doi.org/10.1007/BF02877748>.
 31. Dobryakova, N. V., Zhdanov, D. D., Sokolov, N. N., Aleksandrova, S. S., Pokrovskaya, M. V., and Kudryashova, E. V. (2022) Improvement of biocatalytic properties and cytotoxic activity of L-asparaginase from *Rhodospirillum rubrum* by conjugation with chitosan-based cationic polyelectrolytes, *Pharmaceuticals*, **15**, 406, <https://doi.org/10.3390/ph15040406>.
 32. Imam, H. T., Marr, P. C., and Marr, A. C. (2021) Enzyme entrapment, biocatalyst immobilization without covalent attachment, *Green Chem.*, **23**, 4980-5005, <https://doi.org/10.1039/D1GC01852C>.
 33. Zalewska-Szewczyk, B., Gach, A., Wyka, K., Bodalski, J., and Młynarski, W. (2009) The cross-reactivity of anti-asparaginase antibodies against different l-asparaginase preparations, *Clin. Exp. Med.*, **9**, 113-116, <https://doi.org/10.1007/s10238-008-0026-9>.
 34. Wang, N., Ji, W., Wang, L., Wu, W., Zhang, W., Wu, Q., Du, W., Bai, H., Peng, B., Ma, B., and Li, L. (2022) Overview of the structure, side effects, and activity assays of L-asparaginase as a therapy drug of acute lymphoblastic leukemia, *RSC Med. Chem.*, **13**, 117-128, <https://doi.org/10.1039/D1MD00344E>.
 35. Liang, S. (2023) Advances in drug delivery applications of modified bacterial cellulose-based materials, *Front. Bioeng. Biotechnol.*, **11**, 1252706, <https://doi.org/10.3389/fbioe.2023.1252706>.
 36. Shah, N., Ul-Islam, M., Khattak, W. A., and Park, J. K. (2013) Overview of bacterial cellulose composites: a multipurpose advanced material, *Carbohydr. Polym.*, **98**, 1585-1598, <https://doi.org/10.1016/j.carbpol.2013.08.018>.
 37. Adepu, S., and Khandelwal, M. (2020) *Ex-situ* modification of bacterial cellulose for immediate and sustained drug release with insights into release mechanism, *Carbohydr. Polym.*, **249**, 116816, <https://doi.org/10.1016/j.carbpol.2020.116816>.
 38. Gregory, D. A., Tripathi, L., Fricker, A. T. R., Asare, E., Orlando, I., Raghavendran, V., and Roy, I. (2021) Bacterial cellulose: a smart biomaterial with diverse applications, *Mater. Sci. Eng. R Reports*, **145**, 100623, <https://doi.org/10.1016/j.mser.2021.100623>.
 39. Stumpf, T. R., Yang, X., Zhang, J., and Cao, X. (2018) *In situ* and *ex situ* modifications of bacterial cellulose for applications in tissue engineering, *Mater. Sci. Eng. C*, **82**, 372-383, <https://doi.org/10.1016/j.msec.2016.11.121>.
 40. Cacicedo, M. L., Islan, G. A., León, I. E., Álvarez, V. A., Chourpa, I., Allard-Vannier, E., García-Aranda, N., Díaz-Riascos, Z. V., Fernández, Y., Schwartz, S., Jr., Abasolo, I., and Castro, G. R. (2018) Bacterial cellulose hydrogel loaded with lipid nanoparticles for localized cancer treatment, *Colloids Surfaces B Biointerfaces*, **170**, 596-608, <https://doi.org/10.1016/j.colsurfb.2018.06.056>.
 41. Autier, L., Clavreul, A., Cacicedo, M. L., Franconi, F., Sindji, L., Rousseau, A., Perrot, R., Montero-Menei, C. N.,

- Castro, G. R., and Menei, P. (2019) A new glioblastoma cell trap for implantation after surgical resection, *Acta Biomater.*, **84**, 268-279, <https://doi.org/10.1016/j.actbio.2018.11.027>.
42. Pandey, A., Singh, M. K., and Singh, A. (2024) Bacterial cellulose: a smart biomaterial for biomedical applications, *J. Mater. Res.*, **39**, 2-18, <https://doi.org/10.1557/s43578-023-01116-4>.
43. Pavaloiu, R.-D., Stoica-Guzun, A., Stroescu, M., Jinga, S. I., and Dobre, T. (2014) Composite films of poly(vinyl alcohol)-chitosan-bacterial cellulose for drug controlled release, *Int. J. Biol. Macromol.*, **68**, 117-124, <https://doi.org/10.1016/j.ijbiomac.2014.04.040>.
44. Mohamed, M. H., Udoetok, I. A., Wilson, L. D., and Headley, J. V. (2015) Fractionation of carboxylate anions from aqueous solution using chitosan cross-linked sorbent materials, *RSC Adv.*, **5**, 82065-82077, <https://doi.org/10.1039/C5RA13981C>.
45. Udoetok, I. A., Dimmick, R. M., Wilson, L. D., and Headley, J. V. (2016) Adsorption properties of cross-linked cellulose-epichlorohydrin polymers in aqueous solution, *Carbohydr. Polym.*, **136**, 329-340, <https://doi.org/10.1016/j.carbpol.2015.09.032>.
46. Mohamed, M. H., and Wilson, L. D. (2016) Sequestration of agrochemicals from aqueous media using cross-linked chitosan-based sorbents, *Adsorption*, **22**, 1025-1034, <https://doi.org/10.1007/s10450-016-9796-7>.
47. Wilson, L. D., and Xue, C. (2013) Macromolecular sorbent materials for urea capture, *J. Appl. Polym. Sci.*, **128**, 667-675, <https://doi.org/10.1002/app.38247>.
48. Poon, L., Wilson, L. D., and Headley, J. V. (2014) Chitosan-glutaraldehyde copolymers and their sorption properties, *Carbohydr. Polym.*, **109**, 92-101, <https://doi.org/10.1016/j.carbpol.2014.02.086>.
49. Udoetok, I. A., Wilson, L. D., and Headley, J. V. (2016) Self-assembled and cross-linked animal and plant-based polysaccharides: chitosan-cellulose composites and their anion uptake properties, *ACS Appl. Mater. Interfaces*, **8**, 33197-33209, <https://doi.org/10.1021/acsami.6b11504>.
50. Udoetok, I. A., Wilson, L. D., and Headley, J. V. (2018) "Pillaring Effects" in cross-linked cellulose biopolymers: a study of structure and properties, *Int. J. Polym. Sci.*, **2018**, 6358254, <https://doi.org/10.1155/2018/6358254>.
51. Kim, H. J., Jin, J. N., Kan, E., Kim, K. J., and Lee, S. H. (2017) Bacterial cellulose-chitosan composite hydrogel beads for enzyme immobilization, *Biotechnol. Bioprocess Eng.*, **22**, 89-94, <https://doi.org/10.1007/s12257-016-0381-4>.
52. Ribeiro-Viana, R. M., Faria-Tischer, P. C. S., and Tischer, C. A. (2016) Preparation of succinylated cellulose membranes for functionalization purposes, *Carbohydr. Polym.*, **148**, 21-28, <https://doi.org/10.1016/j.carbpol.2016.04.033>.
53. Wacker, M., Riedel, J., Walles, H., Scherner, M., Awad, G., Varghese, S., Schürlein, S., Garke, B., Veluswamy, P., Wippermann, J., and Hülsmann, J. (2021) Comparative evaluation on impacts of fibronectin, heparin-chitosan, and albumin coating of bacterial nanocellulose small-diameter vascular grafts on endothelialization *in vitro*, *Nanomaterials*, **11**, 1952, <https://doi.org/10.3390/nano11081952>.
54. Jantarat, C., Attakitmongkol, K., Nicksapa, S., Sirathanarun, P., and Srivaro, S. (2020) Molecularly imprinted bacterial cellulose for sustained-release delivery of quercetin, *J. Biomater. Sci. Polym. Ed.*, **31**, 1961-1976, <https://doi.org/10.1080/09205063.2020.1787602>.
55. Arikibe, J. E., Lata, R., Kuboyama, K., Ougizawa, T., and Rohindra, D. (2019) pH-responsive studies of bacterial cellulose/chitosan hydrogels crosslinked with genipin: swelling and drug release behaviour, *ChemistrySelect*, **4**, 9915-9926, <https://doi.org/10.1002/slct.201902290>.
56. Mohammadi, S., Jabbari, F., and Babaeipour, V. (2023) Bacterial cellulose-based composites as vehicles for dermal and transdermal drug delivery: a review, *Int. J. Biol. Macromol.*, **242**, 124955, <https://doi.org/10.1016/j.ijbiomac.2023.124955>.
57. Pasaribu, K. M., Ilyas, S., Tamrin, T., Radecka, I., Swingler, S., Gupta, A., Stamboulis, A. G., and Gea, S. (2023) Bioactive bacterial cellulose wound dressings for burns with collagen *in-situ* and chitosan *ex-situ* impregnation, *Int. J. Biol. Macromol.*, **230**, 123118, <https://doi.org/10.1016/j.ijbiomac.2022.123118>.
58. Abu Hasan, N. S., Mohamad, S., Sy Mohamad, S. F., Arzmi, M. H., and Supian, N. N. I. (2023) *Ex-situ* development and characterization of composite film based on bacterial cellulose derived from oil palm frond juice and chitosan as food packaging, *Pertanika J. Sci. Technol.*, **31**, 1173-1187, <https://doi.org/10.47836/pjst.31.3.03>.
59. Kitaoka, K., Yamamoto, H., Tani, T., Hoshijima, K., and Nakauchi, M. (1997) Mechanical strength and bone bonding of a titanium fiber mesh block for intervertebral fusion, *J. Orthop. Sci.*, **2**, 106-113, <https://doi.org/10.1007/BF02489521>.
60. Wu, S., Wu, S., and Su, F. (2017) Novel process for immobilizing an enzyme on a bacterial cellulose membrane through repeated absorption, *J. Chem. Technol. Biotechnol.*, **92**, 109-114, <https://doi.org/10.1002/jctb.4994>.
61. Isobe, N., Lee, D.-S., Kwon, Y.-J., Kimura, S., Kuga, S., Wada, M., and Kim, U.-J. (2011) Immobilization of protein on cellulose hydrogel, *Cellulose*, **18**, 1251-1256, <https://doi.org/10.1007/s10570-011-9561-8>.
62. Krasotkina, J., Borisova, A. A., Gervaziev, Y. V., and Sokolov, N. N. (2004) One-step purification and kinetic properties of the recombinant L-asparaginase from *Erwinia carotovora*, *Biotechnol. Appl. Biochem.*, **39**, 215-221, <https://doi.org/10.1042/BA20030138>.

63. Dawson, R. M. C., Elliott, D. C., Elliott, W. H., and Jones, K. M. (1989) *Data for Biochemical Research*, 3rd ed. Oxford, Clarendon Press.
64. Meister, A. (1955) Glutaminase, asparaginase, and α -keto acid- ω -amidase, *Methods Enzym.*, **2**, 380-385, [https://doi.org/10.1016/S0076-6879\(55\)02216-7](https://doi.org/10.1016/S0076-6879(55)02216-7).
65. Cooney, D. A., Capizzi, R. L., and Handschumacher, R. E. (1970) Evaluation of L-asparagine metabolism in animals and man, *Cancer Res.*, **30**, 925-935.
66. Dave, P. N., Macwan, P. M., and Kamaliya, B. (2023) Biodegradable Gg-cl-poly(NIPAm-co-AA)/-o-MWCNT based hydrogel for combined drug delivery system of metformin and sodium diclofenac: *in vitro* studies, *RSC Adv.*, **13**, 22875-22885, <https://doi.org/10.1039/D3RA04728H>.
67. Looi, C. Y., Moharram, B., Paydar, M., Wong, Y. L., Leong, K. H., Mohamad, K., Arya, A., Wong, W. F., and Mustafa, M. R. (2013) Induction of apoptosis in melanoma A375 cells by a chloroform fraction of *Centrathrum anthelminticum* (L.) seeds involves NF-kappaB, p53 and Bcl-2-controlled mitochondrial signaling pathways, *BMC Complement. Altern. Med.*, **13**, 166, <https://doi.org/10.1186/1472-6882-13-166>.
68. Denizot, F., and Lang, R. (1986) Rapid colorimetric assay for cell growth and survival, *J. Immunol. Methods*, **89**, 271-277, [https://doi.org/10.1016/0022-1759\(86\)90368-6](https://doi.org/10.1016/0022-1759(86)90368-6).
69. Horue, M., Silva, J. M., Berti, I. R., Brandão, L. R., da Silva Barud, H., and Castro, G. R. (2023) Bacterial cellulose-based materials as dressings for wound healing, *Pharmaceutics*, **15**, 424, <https://doi.org/10.3390/pharmaceutics15020424>.
70. Ul-Islam, M., Khan, T., and Park, J. K. (2012) Water holding and release properties of bacterial cellulose obtained by *in situ* and *ex situ* modification, *Carbohydr. Polym.*, **88**, 596-603, <https://doi.org/10.1016/j.carbpol.2012.01.006>.
71. Li, G., Nandgaonkar, A. G., Habibi, Y., Krause, W. E., Wei, Q., and Lucia, L. A. (2017) An environmentally benign approach to achieving vectorial alignment and high microporosity in bacterial cellulose/chitosan scaffolds, *RSC Adv.*, **7**, 13678-13688, <https://doi.org/10.1039/C6RA26049G>.
72. Li, Y., Jiang, H., Zheng, W., Gong, N., Chen, L., Jiang, X., and Yang, G. (2015) Bacterial cellulose-hyaluronan nanocomposite biomaterials as wound dressings for severe skin injury repair, *J. Mater. Chem. B*, **3**, 3498-3507, <https://doi.org/10.1039/C4TB01819B>.
73. Ul-Islam, M., Shah, N., Ha, J. H., and Park, J. K. (2011) Effect of chitosan penetration on physico-chemical and mechanical properties of bacterial cellulose, *Korean J. Chem. Eng.*, **28**, 1736-1743, <https://doi.org/10.1007/s11814-011-0042-4>.
74. Ojagh, S. M. A., Vahabzadeh, F., and Karimi, A. (2021) Synthesis and characterization of bacterial cellulose-based composites for drug delivery, *Carbohydr. Polym.*, **273**, 118587, <https://doi.org/10.1016/j.carbpol.2021.118587>.
75. Bayer, I. S. (2023) Controlled drug release from nano-engineered polysaccharides, *Pharmaceutics*, **15**, 1364, <https://doi.org/10.3390/pharmaceutics15051364>.
76. Zhu, W., Long, J., and Shi, M. (2023) Release kinetics model fitting of drugs with different structures from viscose fabric, *Materials (Basel)*, **16**, 3282, <https://doi.org/10.3390/ma16083282>.
77. Fu, Y., and Kao, W. J. (2010) Drug release kinetics and transport mechanisms of non-degradable and degradable polymeric delivery systems, *Expert Opin. Drug Deliv.*, **7**, 429-444, <https://doi.org/10.1517/17425241003602259>.
78. Hu, Y., Catchmark, J. M., Zhu, Y., Abidi, N., Zhou, X., Wang, J., and Liang, N. (2014) Engineering of porous bacterial cellulose toward human fibroblasts in-growth for tissue engineering, *J. Mater. Res.*, **29**, 2682-2693, <https://doi.org/10.1557/jmr.2014.315>.
79. Rebelo, A. R., Archer, A. J., Chen, X., Liu, C., Yang, G., and Liu, Y. (2018) Dehydration of bacterial cellulose and the water content effects on its viscoelastic and electrochemical properties, *Sci. Technol. Adv. Mater.*, **19**, 203-211, <https://doi.org/10.1080/14686996.2018.1430981>.
80. Numata, Y., Kono, H., Mori, A., Kishimoto, R., and Tajima, K. (2019) Structural and rheological characterization of bacterial cellulose gels obtained from *Gluconacetobacter* genus, *Food Hydrocoll.*, **92**, 233-239, <https://doi.org/10.1016/j.foodhyd.2019.01.060>.
81. Munim, S. A., Saddique, M. T., Raza, Z. A., and Majeed, M. I. (2020) Fabrication of cellulose-mediated chitosan adsorbent beads and their surface chemical characterization, *Polym. Bull.*, **77**, 183-196, <https://doi.org/10.1007/s00289-019-02711-4>.
82. Urbina, L., Guaresti, O., Requies, J., Gabilondo, N., Eceiza, A., Corcuera, M. A., and Retegi, A. (2018) Design of reusable novel membranes based on bacterial cellulose and chitosan for the filtration of copper in wastewaters, *Carbohydr. Polym.*, **193**, 362-372, <https://doi.org/10.1016/j.carbpol.2018.04.007>.
83. Kalyani, P., and Khandelwal, M. (2021) Modulation of morphology, water uptake/retention, and rheological properties by *in situ* modification of bacterial cellulose with the addition of biopolymers, *Cellulose*, **28**, 11025-11036, <https://doi.org/10.1007/s10570-021-04256-0>.
84. Maity, M., Pramanik, U., Hathwar, V. R., Brandao, P., Mukherjee, S., Maity, S., Maity, R., Maity, T., and Chandra Samanta, B. (2022) Biophysical insights into the binding capability of Cu(II) schiff base complex with BSA protein and cytotoxicity studies against SiHa, *Heliyon*, **8**, e11345, <https://doi.org/10.1016/j.heliyon.2022.e11345>.
85. Monteiro, O. A., and Airoidi, C. (1999) Some studies of crosslinking chitosan-glutaraldehyde interaction in

- a homogeneous system, *Int. J. Biol. Macromol.*, **26**, 119-128, [https://doi.org/10.1016/S0141-8130\(99\)00068-9](https://doi.org/10.1016/S0141-8130(99)00068-9).
86. Vasconcellos, V., and Farinas, C. (2018) The effect of the drying process on the properties of bacterial cellulose films from *Gluconacetobacter hansenii*, *Chem. Eng. Trans.*, **64**, 145-150, <https://doi.org/10.3303/CET1864025>.
87. Ciecholewska-Juško, D., Żywicka, A., Junka, A., Drozd, R., Sobolewski, P., Migdał, P., Kowalska, U., Toporkiewicz, M., and Fijałkowski, K. (2021) Superabsorbent crosslinked bacterial cellulose biomaterials for chronic wound dressings, *Carbohydr. Polym.*, **253**, 117247, <https://doi.org/10.1016/j.carbpol.2020.117247>.
88. Ciecholewska-Juško, D., Junka, A., and Fijałkowski, K. (2022) The cross-linked bacterial cellulose impregnated with octenidine dihydrochloride-based antiseptic as an antibacterial dressing material for highly-exuding, infected wounds, *Microbiol. Res.*, **263**, 127125, <https://doi.org/10.1016/j.micres.2022.127125>.
89. Wahid, F., Hu, X.-H., Chu, L.-Q., Jia, S.-R., Xie, Y.-Y., and Zhong, C. (2019) Development of bacterial cellulose/chitosan based semi-interpenetrating hydrogels with improved mechanical and antibacterial properties, *Int. J. Biol. Macromol.*, **122**, 380-387, <https://doi.org/10.1016/j.ijbiomac.2018.10.105>.
90. Li, J., and Mooney, D. J. (2016) Designing hydrogels for controlled drug delivery, *Nat. Rev. Mater.*, **1**, 16071, <https://doi.org/10.1038/natrevmats.2016.71>.
91. Kim, J., Cai, Z., Lee, H. S., Choi, G. S., Lee, D. H., and Jo, C. (2011) Preparation and characterization of a Bacterial cellulose/Chitosan composite for potential biomedical application, *J. Polym. Res.*, **18**, 739-744, <https://doi.org/10.1007/s10965-010-9470-9>.
92. Lin, W.-C., Lien, C.-C., Yeh, H.-J., Yu, C.-M., and Hsu, S. (2013) Bacterial cellulose and bacterial cellulose-chitosan membranes for wound dressing applications, *Carbohydr. Polym.*, **94**, 603-611, <https://doi.org/10.1016/j.carbpol.2013.01.076>.
93. Shishparenok, A. N., Koroleva, S. A., Dobryakova, N. V., Gladilina, Y. A., Gromovykh, T. I., Solopov, A. B., Kudryashova, E. V., and Zhdanov, D. D. (2024) Bacterial cellulose films for L-asparaginase delivery to melanoma cells, *Int. J. Biol. Macromol.*, **276**, 133932, <https://doi.org/10.1016/j.ijbiomac.2024.133932>.
94. Paul, D. R. (2011) Elaborations on the Higuchi model for drug delivery, *Int. J. Pharm.*, **418**, 13-17, <https://doi.org/10.1016/j.ijpharm.2010.10.037>.
95. Siepmann, J., and Peppas, N. A. (2011) Higuchi equation: derivation, applications, use and misuse, *Int. J. Pharm.*, **418**, 6-12, <https://doi.org/10.1016/j.ijpharm.2011.03.051>.
96. Danyuo, Y., Ani, C. J., Salifu, A. A., Obayemi, J. D., Dozie-Nwachukwu, S., Obanawu, V. O., Akpan, U. M., Odusanya, O. S., Abade-Abugre, M., McBagonluri, F., and Soboyejo, W. O. (2019) Anomalous release kinetics of prodigiosin from poly-N-isopropyl-acrylamid based hydrogels for the treatment of triple negative breast cancer, *Sci. Rep.*, **9**, 3862, <https://doi.org/10.1038/s41598-019-39578-4>.
97. Drozd, R., Szymańska, M., Przygrodzka, K., Hoppe, J., Leniec, G., and Kowalska, U. (2021) The simple method of preparation of highly carboxylated bacterial cellulose with Ni- and Mg-ferrite-based versatile magnetic carrier for enzyme immobilization, *Int. J. Mol. Sci.*, **22**, 8563, <https://doi.org/10.3390/ijms22168563>.
98. Ciolacu, D. E., Nicu, R., and Ciolacu, F. (2020) Cellulose-based hydrogels as sustained drug-delivery systems, *Materials (Basel)*, **13**, 5270, <https://doi.org/10.3390/ma13225270>.
99. Kislyak, I. A., Pokrovskaya, M. V., Zhanturina, D. Y., and Pokrovsky, V. S. (2023) The use of L-asparaginase for the treatment of solid tumors: data from experimental studies and clinical trials, *Russ. J. Oncol.*, **28**, 79-94, <https://doi.org/10.17816/onco562802>.
100. Taylor, C. W., Dorr, R. T., Fanta, P., Hersh, E. M., and Salmon, S. E. (2001) A phase I and pharmacodynamic evaluation of polyethylene glycol-conjugated L-asparaginase in patients with advanced solid tumors, *Cancer Chemother. Pharmacol.*, **47**, 83-88, <https://doi.org/10.1007/s002800000207>.
101. Nerkar, D. P., and Gangadharan, M. (1989) Modification of L-asparaginase from *Erwinia carotovora* using human serum albumin, *Mol. Biother.*, **1**, 152-154.
102. Sukhoverkov, K. V., and Kudryashova, E. V. (2015) PEG-chitosan and glycol-chitosan for improvement of biopharmaceutical properties of recombinant L-asparaginase from *Erwinia carotovora*, *Biochemistry (Moscow)*, **80**, 113-119, <https://doi.org/10.1134/S0006297915010137>.
103. Sukhoverkov, K. V., Sokolov, N. N., Abakumova, O. Y., Podobed, O. V., and Kudryashova, E. V. (2016) The formation of conjugates with PEG-chitosan improves the biocatalytic efficiency and antitumor activity of L-asparaginase from *Erwinia carotovora*, *Moscow Univ. Chem. Bull.*, **71**, 122-126, <https://doi.org/10.3103/S0027131416020073>.
104. Rossi, L., Pierigè, F., Aliano, M. P., and Magnani, M. (2020) Ongoing developments and clinical progress in drug-loaded red blood cell technologies, *BioDrugs*, **34**, 265-272, <https://doi.org/10.1007/s40259-020-00415-0>.
105. Burke, M. J., and Zalewska-Szewczyk, B. (2022) Hypersensitivity reactions to asparaginase therapy in acute lymphoblastic leukemia: immunology and Clinical consequences, *Futur. Oncol.*, **18**, 1285-1299, <https://doi.org/10.2217/fon-2021-1288>.
106. Villani, A., Potestio, L., Fabbrocini, G., Troncone, G., Malapelle, U., and Scalvenzi, M. (2022) The treatment of advanced melanoma: therapeutic update, *Int. J. Mol. Sci.*, **23**, 6388, <https://doi.org/10.3390/ijms23126388>.
107. Klinac, D., Gray, E. S., Millward, M., and Ziman, M. (2013) Advances in personalized targeted treatment of metastatic melanoma and non-invasive tumor

- monitoring, *Front. Oncol.*, **3**, 54, <https://doi.org/10.3389/fonc.2013.00054>.
108. Pokrovsky, V. S., Chepikova, O. E., Davydov, D. Z., Zamyatnin, A. A., Jr., Lukashev, A. N., and Lukasheva, E. V. (2019) Amino acid degrading enzymes and their application in cancer therapy, *Curr. Med. Chem.*, **26**, 446-464, <https://doi.org/10.2174/0929867324666171006132729>.
109. Pokrovsky, V. S., Abo Qoura, L., Morozova, E., and Bunik, V. I. (2022) Predictive markers for efficiency of the amino-acid deprivation therapies in cancer, *Front. Med.*, **9**, 1035356, <https://doi.org/10.3389/fmed.2022.1035356>.
110. Vishnubhakthula, S., Elupula, R., and Durán-Lara, E. F. (2017) Recent advances in hydrogel-based drug delivery for melanoma cancer therapy: a mini review, *J. Drug Deliv.*, **2017**, 7275985, <https://doi.org/10.1155/2017/7275985>.
111. Rastogi, V., and Yadav, P. (2012) Transdermal drug delivery system: an overview, *Asian J. Pharm.*, **6**, 161, <https://doi.org/10.4103/0973-8398.104828>.
112. Ramadan, D., McCrudden, M. T. C., Courtenay, A. J., and Donnelly, R. F. (2022) Enhancement strategies for transdermal drug delivery systems: current trends and applications, *Drug Deliv. Transl. Res.*, **12**, 758-791, <https://doi.org/10.1007/s13346-021-00909-6>.
113. Kalluri, H., and Banga, A. K. (2011) Transdermal delivery of proteins, *AAPS PharmSciTech*, **12**, 431-441, <https://doi.org/10.1208/s12249-011-9601-6>.
114. Shakambari, G., Sameer Kumar, R., Ashokkumar, B., Ganesh, V., Vasantha, V. S., and Varalakshmi, P. (2018) Cloning and expression of L-asparaginase from *Bacillus tequilensis* PV9W and therapeutic efficacy of Solid Lipid Particle formulations against cancer, *Sci. Rep.*, **8**, 18013, <https://doi.org/10.1038/s41598-018-36161-1>.
115. Zhdanov, D. D., Pokrovsky, V. S., Pokrovskaya, M. V., Alexandrova, S. S., Eldarov, M. A., Grishin, D. V., Basharov, M. M., Gladilina, Y. A., Podobed, O. V., and Sokolov, N. N. (2017) *Rhodospirillum rubrum* L-asparaginase targets tumor growth by a dual mechanism involving telomerase inhibition, *Biochem. Biophys. Res. Commun.*, **492**, 282-288, <https://doi.org/10.1016/j.bbrc.2017.08.078>.
116. Zhdanov, D. D., Pokrovsky, V. S., Pokrovskaya, M. V., Alexandrova, S. S., Eldarov, M. A., Grishin, D. V., Basharov, M. M., Gladilina, Y. A., Podobed, O. V., and Sokolov, N. N. (2017) Inhibition of telomerase activity and induction of apoptosis by *Rhodospirillum rubrum* L-asparaginase in cancer Jurkat cell line and normal human CD4⁺ T lymphocytes, *Cancer Med.*, **6**, 2697-2712, <https://doi.org/10.1002/cam4.1218>.
117. Plyasova, A. A., Pokrovskaya, M. V., Lisitsyna, O. M., Pokrovsky, V. S., Alexandrova, S. S., Hilal, A., Sokolov, N. N., and Zhdanov, D. D. (2020) Penetration into cancer cells via clathrin-dependent mechanism allows l-asparaginase from *Rhodospirillum rubrum* to inhibit telomerase, *Pharmaceuticals*, **13**, 286, <https://doi.org/10.3390/ph13100286>.
118. Bosmann, H. B., and Kessel, D. (1970) Inhibition of glycoprotein synthesis in L5178Y mouse leukemic cells by L-asparaginase *in vitro*, *Nature*, **226**, 850-851, <https://doi.org/10.1038/226850a0>.
119. Ankel, E. G., Zirneski, J., Ring, B. J., and Holcenberg, J. S. (1984) Effect of asparaginase on cell membranes of sensitive and resistant mouse lymphoma cells, *In Vitro*, **20**, 376-384, <https://doi.org/10.1007/BF02619582>.
120. Dumina, M. V., Zhgun, A. A., Pokrovskaya, M. V., Alexandrova, S. S., Zhdanov, D. D., Sokolov, N. N., and El'darov, M. A. (2021) Comparison of enzymatic activity of novel recombinant L-asparaginases of extremophiles, *Appl. Biochem. Microbiol.*, **57**, 594-602, <https://doi.org/10.1134/S0003683821050057>.
121. Dumina, M., Zhgun, A., Pokrovskaya, M., Aleksandrova, S., Zhdanov, D., Sokolov, N., and El'darov, M. (2021) A novel L-asparaginase from hyperthermophilic archaeon *Thermococcus sibiricus*: heterologous expression and characterization for biotechnology application, *Int. J. Mol. Sci.*, **22**, 9894, <https://doi.org/10.3390/ijms22189894>.
122. Dumina, M., Zhgun, A., Pokrovskaya, M., Aleksandrova, S., Zhdanov, D., Sokolov, N., and El'darov, M. (2021) Highly active thermophilic L-asparaginase from *Meliolibacter roseus* represents a novel large group of type II bacterial L-asparaginases from chlorobionobacteria-bacteroidetes clade, *Int. J. Mol. Sci.*, **22**, 13632, <https://doi.org/10.3390/ijms222413632>.

Publisher's Note. Pleiades Publishing remains neutral with regard to jurisdictional claims in published maps and institutional affiliations. AI tools may have been used in the translation or editing of this article.